ELSEVIER

International Journal of Pharmaceutics 170 (1998) 93–108

international journal of pharmaceutics

Lag time data for characterizing the pore pathway of intact and chemically pretreated human epidermal membrane

S. Kevin Li *, Wonhee Suh, Hemanshu H. Parikh, Abdel-Halim Ghanem, Samir C. Mehta, Kendall D. Peck, William I. Higuchi

Department of Pharmaceutics and Pharmaceutical Chemistry, 301 Skaggs Hall, University of Utah, Salt Lake City, UT 84112, USA

Received 18 September 1997; received in revised form 24 February 1998; accepted 2 April 1998

Abstract

This study aimed to gain mechanistic insights into the nature of the pore pathway of fully hydrated human stratum corneum from lag time data obtained using a model polar permeant, urea. Lag times were deduced from transport experiments with human epidermal membranes and with human epidermal membranes after ethanol or chloroform–methanol treatment. A tortuous pore pathway transport model and a 'bottleneck' transport model were employed for data analysis, and their appropriateness for the observed data was examined. Important outcomes from the present study with intact and with delipidized stratum corneum were as follows. Long lag times (around 60–800 min) for the transport of urea in human epidermal membranes were generally observed. These results were consistent with an extremely tortuous pore pathway as would be expected if it is associated with the polar/aqueous region of the stratum corneum intercellular lipids (i.e. the bilayers in the intercellular region). The permeability of the stratum corneum increased after ethanol treatment, and, at the same time, the tortuosity decreased but remained relatively high. Chloroform–methanol treatment further increased the permeability and further decreased the tortuosity. Since delipidization by ethanol and chloroform–methanol treatments decreased the tortuosity of the pore pathway, these results suggest that the effectively highly tortuous pathway for polar permeants in stratum corneum may be associated with the polar regions of the intercellular lipids. Untreated skin samples that had high electrical resistance were observed to have longer lag times than those with low resistance; this is consistent with the hypothesis that skin samples of high resistance have less appendage routes or less damage and transport polar permeants predominantly via the tortuous pathways involving the intercellular lipid regions of the stratum corneum. Neither the tortuous pathway transport model alone nor the 'bottleneck' transport model alone seems to perfectly represent the experimental data, and a modified model (a hybrid of the two models) has been proposed to be more consistent with the lag time data and the morphology of fully hydrated stratum corneum. The present study has demonstrated the usefulness of lag times obtained with a polar permeant in better understanding the transport mechanisms involved with the pore pathway.

* Corresponding author. Tel.: +1 801 5814110; e-mail: kevin.li@m.cc.utah.edu

0378-5173/98/$19.00
PII S0378-5173(98)00139-2

Keywords: Human epidermal membrane; Lag time; Penetration enhancers; Permeation; Pore pathway

1. Introduction

The barrier properties of human skin have been studied extensively in attempts to understand the mechanisms of drug transport across skin. The transport of polar compounds across skin has been of particular interest to pharmaceutical scientists because of the low permeability of skin to such permeants and the need to know of methods for enhancing the transport of such compounds across skin. Previously, the importance of considering a pore pathway in any model to describe the transport of polar compounds across the skin and the inadequacy of using a model involving only a lipoidal pathway to describe the transport of both lipophilic and polar compounds have been discussed (Ackermann et al., 1987; Morimoto et al., 1992; Hatanaka et al., 1993; Peck et al., 1994, 1995). Despite the evidence supporting the existence of a pore pathway, the need for considering such a pathway to describe the barrier properties of skin has been questioned (Guy and Hadgraft, 1988; Potts and Guy, 1992, 1995). Moreover, the morphological basis for this pathway has remained unclear and somewhat controversial. The nature of the pore pathway has been recently, examined in our laboratory (Peck et al., 1994, 1995) and among the important outcomes of these studies were the demonstration of the aqueous nature of this pathway and the determination of its effective pore size.

Lag time data may offer independent insights into the transport character of a biomembrane. Lag times associated with the transport of lipophilic compounds across stratum corneum (SC) have been previously reported in the literature (Roberts et al., 1977; Loftsson and Bodor, 1981; Tojo et al., 1987; Goto et al., 1993), but it is difficult to learn much about transport mechanisms from such data due to the lack of information on the simultaneous diffusion and partitioning of lipophilic permeants in the complex rate-limiting lipoidal domains of the SC. Polar permeants, on the other hand, are believed to follow aqueous pore pathways in the SC (Flynn, 1990; Hatanaka et al., 1994; Peck et al., 1995), with the lipoidal domains being largely obstacles around which, or structures with aqueous channels in which the permeants may partition and diffuse. Thus, relatively speaking, SC lag time data obtained with polar permeants are expected to be more amenable to interpretation, with the principal parameters being porosity and tortuosity. Accordingly, the focus of the present study was to examine the use of lag times of polar permeants with human epidermal membrane (HEM) as a means to characterize and to better understand the nature of the pore pathway of fully hydrated human SC.

2. Materials and methods

2.1. Materials

[^{14}C]Urea was obtained from New England Nuclear (Boston, MA). Human epidermal membrane (HEM) was provided by TheraTech Inc. (Salt Lake City, UT). The epidermal membrane was prepared by heat separation using human skin removed from the back, abdomen or thigh as previously described (Sims et al., 1991), and immediately frozen for later use. Phosphate-buffered saline with 0.02% sodium azide (PBS), ionic strength 0.10 M and pH 7.4, was prepared from reagent grade chemicals and distilled deionized water (Li et al., 1997). Methanol (MeOH) and chloroform ($CHCl_3$) were purchased at HPLC grade. Millipore GVWP filters were obtained from Millipore (Bedford, MA).

2.2. Permeation studies

Permeation studies were conducted in side-by-side diffusion cells (with a diffusional area of

around 0.75 cm^2) filled with PBS and maintained at 37°C in a circulating waterbath. An experimental protocol was followed which utilized the same sample of HEM both in the standard permeation experiments and in the pretreatment/transport experiments. HEM samples were mounted with a Millipore filter membrane between the half-cells as described previously (Peck et al., 1993), and were allowed to reach equilibrium in PBS at 37°C for 30–48 h before initiating the permeability runs. The electrical conductance of HEM usually decreased or sometime increased during this equilibration period but generally did not change by more than 50%. In each experiment, the receiver and donor chambers were filled with PBS and PBS pre-mixed with a trace amount of radiolabeled urea, respectively. At predetermined intervals, 1 ml samples were withdrawn from the receiver chamber and replaced with fresh PBS. At the same time, 10-μl samples were also withdrawn from the donor chamber. The samples were then mixed with 10 ml of scintillation cocktail (Ultima Gold™; Packard, Meriden, CT) and assayed in a liquid scintillation counter. The permeability coefficient (P) was calculated from the steady-state flux as follows:

$$P = \frac{1}{AC_D}\frac{dQ}{dt} \quad (1)$$

where Q is the cumulative amount of the permeant in the receiver chamber, A is the diffusional area, C_D is the concentration of the permeant in the donor chamber, and t is time. The lag time (T) was determined by extrapolating the steady-state data (Q vs. t) to the abscissa (e.g. Martin and Bustamante, 1993). The electrical resistance of HEM was checked periodically by a four-electrode potentiostat system with a voltage drop of 100 mV. The four-electrode potentiostat system was described previously (Srinivasan et al., 1989), and Ag–AgCl counter electrodes were used. HEM electrical resistance was used to monitor any changes in the HEM barrier during the course of the experiment. Samples with greater than 20% change in electrical resistance during the permeation run were considered unsuitable and were discarded. After the first passive permeation run, some of the HEM samples in the diffusion cells were rinsed with fresh PBS and used in further studies involving treatment with trypsin solution, ethanol (EtOH), or $CHCl_3$–MeOH (2:1, v/v) followed by a second permeation run.

2.3. EtOH, $CHCl_3$–MeOH and trypsin treatments

Ethanol and $CHCl_3$–MeOH pretreatment studies were carried out by equilibrating HEM mounted in a diffusion cell with 100% ethanol or $CHCl_3$–MeOH (2:1, v/v). The diffusion cell was first rinsed with ethanol or $CHCl_3$–MeOH and then filled with the particular solvent. The membrane was then allowed to equilibrate with the particular solvent with stirring at 37°C for 2 h. Following the 2-h treatment, the diffusion cell chambers were rinsed several times with fresh PBS, and the treated HEM was allowed to equilibrate in PBS for 24 h before the permeation experiment. Permeation runs were then conducted at 37°C as described in Section 2.2. Trypsin treatment of HEM was carried out in a similar fashion but with 0.05% trypsin (Sigma, St. Louis, MO) in PBS in the receiver chamber. After the diffusion cell was equilibrated (with stirring) at 37°C for 1 day, the trypsin solution was removed and the cells were rinsed and filled with fresh PBS. The concentration of trypsin chosen was based on results from preliminary studies at different trypsin concentrations (0.001, 0.01, 0.05, and 0.1%). At 0.05% trypsin in PBS, HEM electrical resistance remained essentially unchanged during the treatment, and the viable epidermal layer was observed to have been removed.

2.4. Stratum corneum thickness determination

Trypsin treatment of HEM was conducted as described above by adding trypsin (0.05% or 0.2%) in PBS in the receiver chamber of the diffusion cell and equilibrating for 1 day at 37°C while monitoring the electrical resistance. Another group of HEM samples were soaked in the trypsin in PBS in a Petri dish under normal room conditions for 1 day. The thickness of the trypsin treated HEM from the cells and from the Petri dish was determined with a micrometer as previously described (Pershing et al., 1990).

2.5. Characterization of the Millipore supporting membrane and the unstirred boundary layer

The permeability coefficient of the unstirred boundary layer and that of the Millipore membrane were estimated by conducting transport experiments with a single Millipore membrane and with assemblies of two and five Millipore membranes (from the same lot) in a diffusion cell as described above and using a transport model consisting of membranes in series. The permeability of the Millipore supporting membrane and that of the unstirred boundary layers can be expressed by (Martin and Bustamante, 1993):

$$\frac{1}{P}=\frac{n}{P_{\mathrm{m}}}+\frac{1}{P_{\mathrm{u}}} \tag{2}$$

where P is the experimental permeability coefficient and P_{u} and P_{m} are the permeability coefficients of the unstirred boundary layer and that of a single Millipore membrane, respectively, and n is the number of Millipore membranes in the composite membrane. P_{m} and P_{u} are determined by the slope and intercept of $1/P$ vs. n plot.

2.6. Models

Two transport models, a tortuous pore pathway model and a 'bottleneck' transport model, were considered for the purpose of experimental data analysis in the present study. The tortuous pore pathway model is an explicit, commonly used physical model whereas the 'bottleneck' transport model is more of a phenomenological model. In the tortuous pore pathway model, the tortuosity (τ) and the porosity (ϵ) of the pore pathway and the effective thickness ($h\tau$) of human SC were calculated using the experimental permeability coefficient and the lag time, and Eqs. (3) and (4) (e.g. Flynn et al., 1974; Peck et al., 1994):

$$T=\frac{(h\tau)^2}{6DH} \tag{3}$$

$$P=\frac{\epsilon DH}{h\tau} \tag{4}$$

where D (1.8×10^{-5} cm^2/s for urea; Peck et al., 1994) is the diffusion coefficient, h is the thickness of SC, and H is the hindrance factor for passive diffusion. This model assumes tortuous aqueous circular cylindrical channels of constant cross sectional area with radius of 20 Å in the pore pathways of SC; with urea, $H\approx0.55$ for a 20-Å pore (Peck et al., 1994). This model also assumes zero access of the permeant to any other compartments (e.g. aqueous compartments of the corneocytes or aqueous 'pockets' in the intercellular regions; van Hal et al., 1996).

When significant aqueous compartments (such as those associated with either or both the intercellular lipids and the corneocytes in SC) accessible to the permeants are present in a membrane, longer times would be required to reach steady-state. An extreme of this situation can be described as a 'bottleneck' transport model in which the pore pathway is modeled as a series of aqueous compartments interconnected by transport rate-limiting 'bottlenecks'. In the present context, the size of these aqueous compartments might be associated with the hydration volume for SC, and the pore pathway may be described as a series of j such aqueous compartments separated by transport rate-limiting barriers with permeability, P_{l}. The permeant concentration in each compartment can be expressed as:

$$\frac{\mathrm{d}C_1}{\mathrm{d}t}=\frac{A[P_{\mathrm{l}}(C_{\mathrm{D}}-C_1)-P_{\mathrm{l}}(C_1-C_2)]}{V} \tag{5}$$

for compartment 1, and

$$\frac{\mathrm{d}C_{\mathrm{i}}}{\mathrm{d}t}=\frac{A[P_{\mathrm{l}}(C_{\mathrm{i}-1}-C_{\mathrm{i}})-P_{\mathrm{l}}(C_{\mathrm{i}}-C_{\mathrm{i}+1})]}{V} \tag{6}$$

for compartment i, and

$$\frac{\mathrm{d}C_{\mathrm{j}}}{\mathrm{d}t}=\frac{A[P_{\mathrm{l}}(C_{\mathrm{j}-1}-C_{\mathrm{j}})-P_{\mathrm{l}}C_{\mathrm{j}}]}{V} \tag{7}$$

for compartment j, and

$$\frac{\mathrm{d}Q}{\mathrm{d}t}=AP_{\mathrm{l}}C_{\mathrm{j}} \tag{8}$$

where A is the surface area of the membrane (0.75 cm^2), V is the volume of each aqueous compartment, t is time, Q is the cumulative amount of the permeant in the receiver chamber, C_{i}, C_{j} and C_{D} are the concentrations of the permeant in compartment i, in compartment j, and in

the donor chamber, respectively, and P_l is the permeability coefficient of the barrier between (interconnecting) each compartment. P_l can be described by an equation similar to Eq. (4), and its value estimated by:

$$\frac{1}{P_t} = \frac{j+1}{P_l} \tag{9}$$

where P_t (from around 10^{-8} to 10^{-5} cm/s) is the total permeability coefficient of the membrane. This model assumes that: (1) the lag time for transport between each compartment is relatively insignificant compared with the total transport lag time of the system (e.g. a small $h\tau$ value for the barrier interconnecting each compartment); (2) the aqueous phase in these compartments behaves like bulk water; (3) a constant volume for each compartment; and (4) sink conditions in the receiver chamber. The transport lag time simulations were carried out with Eqs. (5)–(8) using Scientist® (MicroMath Scientific Software Inc., Salt Lake City, UT) with permeability coefficients calculated by Eq. (9) and by varying the volume parameter V.

Although there are possible mechanisms requiring alternative transport models to explain the lag time data, the models for the two extreme cases described above involving Eqs. (3) and (4) and Eqs. (5)–(9) were adopted for simplicity in the present study.

3. Results

3.1. Stratum corneum thickness determination

The thicknesses of trypsin treated HEM were 27 ± 9 μm (mean $\pm$ S.D., $n = 24$), and the electrical resistances of these HEM samples were between 20 and 40 kΩ cm^2. No significant differences in membrane thickness were observed between samples treated in the diffusion cells at 37°C and in the Petri dish under room conditions. Thicknesses of 0.05% and 0.2% trypsin treated HEM were also essentially the same. It should be noted that the results obtained in the present study are in the same order of magnitude with previous findings (Allenby et al., 1969; Pershing et al., 1990; Corcuff et al., 1996). Although variations in SC thickness have been reported for skin samples obtained from different regions of the human body (Holbrook and Odland, 1974), such variations of SC thickness were noted not to be large among the samples removed from the abdomens, forearms, backs and thighs; this is consistent with the relatively constant SC thickness determined with different skin samples in the present study.

3.2. Supporting Millipore membrane and the unstirred boundary layer

The permeability coefficients and transport lag times of the unstirred boundary layer and of the supporting Millipore membrane were estimated by data obtained in the Millipore membrane permeation studies. The permeability coefficient of the unstirred boundary layer (P_u) and that of a single Millipore membrane (P_m) were 9×10^{-4} and 6×10^{-4} cm/s, respectively. The lag time for the combination of the unstirred boundary layer and a supporting Millipore membrane was estimated to be less than around 10 s from the same experiments.

3.3. HEM, EtOH treated HEM and $CHCl_3$–MeOH treated HEM permeation studies

Raw data from typical transport experiments with HEM, with ethanol treated HEM, and with $CHCl_3$–MeOH treated HEM are presented in Figs. 1–3, respectively. The permeability coefficients (P), lag times (T) and electrical resistance (R) for all of the experiments are presented in Table 1. Table 1 shows the long lag times (397 ± 211 min, ranging from around 60 to 800 min) for the transport of urea across fully hydrated SC. A significant decrease in the transport lag times was observed in ethanol and $CHCl_3$–MeOH treated HEM. Also seen in Table 1 is the large increase in P after these solvent treatments. Since ethanol and $CHCl_3$–MeOH treatments have been associated with the removal of SC intercellular lipids (Wertz and Downing, 1986; Bommannan et al., 1991), this increase in P suggests that the rate determining barrier for polar compounds in SC is

Table 1
Permeability coefficient (P), lag time (T) and electrical resistance (R) of HEM, trypsin treated HEM, ethanol (EtOH) treated HEM and $CHCl_3$–MeOH treated HEM

Sample	PBS			Trypsin treated			EtOH treated			$CHCl_3$–MeOH treated		
	P ($\times 10^8$ cm/s)	T (min)	R (kΩ cm^2)	P ($\times 10^8$ cm/s)	T (min)	R (kΩ cm^2)	P ($\times 10^6$ cm/s)	T (min)	R (kΩ cm^2)	P ($\times 10^6$ cm/s)	T (min)	R (kΩ cm^2)
a	3.6	357	51	–	–	–	–	–	–	–	–	–
b	3.0	326	53	–	–	–	–	–	–	–	–	–
c	3.7	286	44	–	–	–	–	–	–	–	–	–
d	2.5	470	58	–	–	–	–	–	–	–	–	–
e	3.5	300	49	–	–	–	–	–	–	–	–	–
f	2.7	372	70	–	–	–	–	–	–	–	–	–
g	3.7	491	35	–	–	–	8.5	6.3	0.37	–	–	–
h	0.91	733	81	–	–	–	5.4	3.3	0.40	–	–	–
i	3.5	363	46	–	–	–	4.1	7.6	0.67	–	–	–
j	7.7	64	16	–	–	–	4.5	10	0.64	–	–	–
k	0.55	850	157	0.68	750	163	21	0.12	0.055	–	–	–
l	1.2	641	94	0.77	583	112	2.5	16	1.0	–	–	–
m	1.8	489	74	2.2	503	64	4.1	15	0.60	–	–	–
n	6.5	237	31	–	–	–	–	–	–	153	0.52	0.023
o	2.8	500	65	–	–	–	–	–	–	145	1.2	0.030
p	18	149	10.5	–	–	–	–	–	–	105	1.1	0.035
q	10.8	123	19	–	–	–	–	–	–	184	0.2	0.025
Mean ± S.D.		397 ± 211						8.3 ± 5.8			0.75 ± 0.48	

No significant changes in the parameters presented in this study were observed for HEM after trypsin treatment. A significant increase in P and a significant decrease in both T and R were observed after ethanol and $CHCl_3$–MeOH treatments.

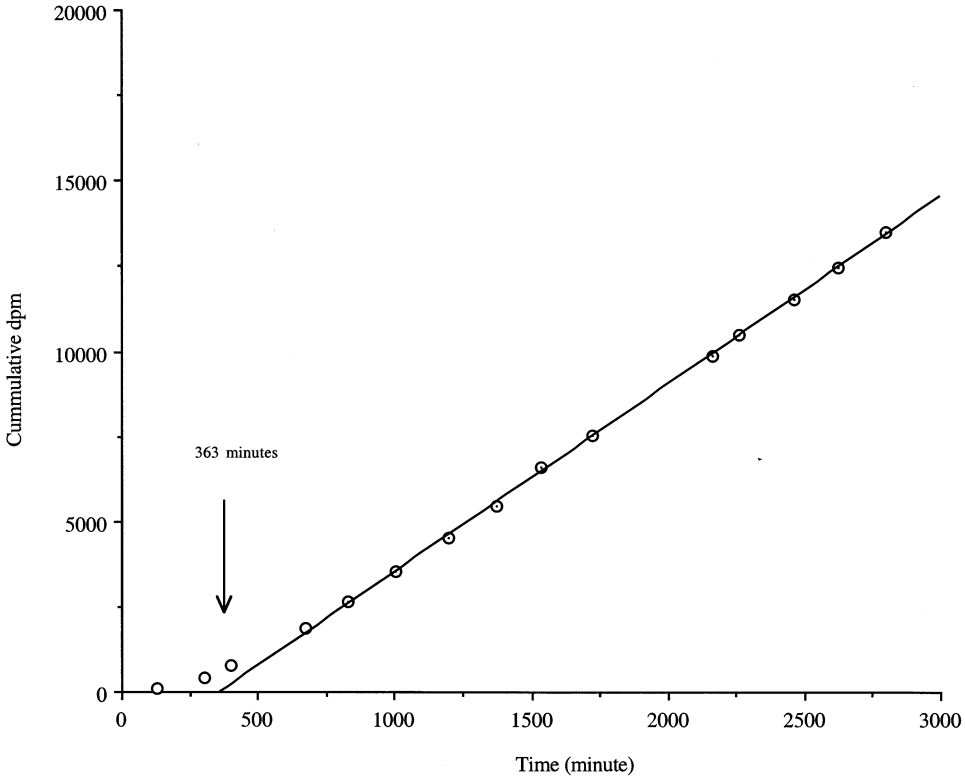

Fig. 1. Representative flux data in a permeation study with HEM (skin sample i). The donor concentration in this permeation experiment was 3.5×10^6 dpm/ml. The slope of the linear regression line is 5.5 dpm/min.

related to its intercellular lipids. One should also note that the P values of $CHCl_3$–MeOH treated HEM begin to approach those determined for the unstirred boundary layer and the Millipore supporting membrane. With these large P values, the barrier function of the viable epidermis would also be expected to become non-negligible relative to that of the SC. Thus, the usefulness of the lag time data in the $CHCl_3$–MeOH pretreatment studies may be questioned, and the results from these studies can only serve as a rough estimate of the HEM permeability behavior after $CHCl_3$–MeOH treatment.

3.4. Results from the tortuous pore pathway model using data obtained in HEM, EtOH treated HEM and $CHCl_3$–MeOH treated HEM permeation studies

The effective thickness ($h\tau$) and porosity (ϵ) for SC were calculated from the P and T values using Eqs. (3) and (4), and the results are given in Table 2. It should be noted that skin samples k, l and m followed a protocol different from that with the other skin samples (skin samples g, h, i and j). Unlike the other skin samples that were treated by ethanol directly after the permeation study in PBS, skin samples k, l and m were treated with trypsin followed by a permeation run before the ethanol treatment. The tortuosity (τ) values were estimated from the $h\tau$ values in Table 2 and with the physical SC thickness (h) of 27 μm for fully hydrated human SC (see Section 3.1). The large τ values found (420 ± 119, ranging from around 180 to 660) suggest highly tortuous pathways for polar permeants in SC. Although the calculated porosity values of SC generally increased by around a factor of 20 (with around a 100-fold increase in P values) after ethanol treatment (see Table 1), the tortuosity values remained relatively

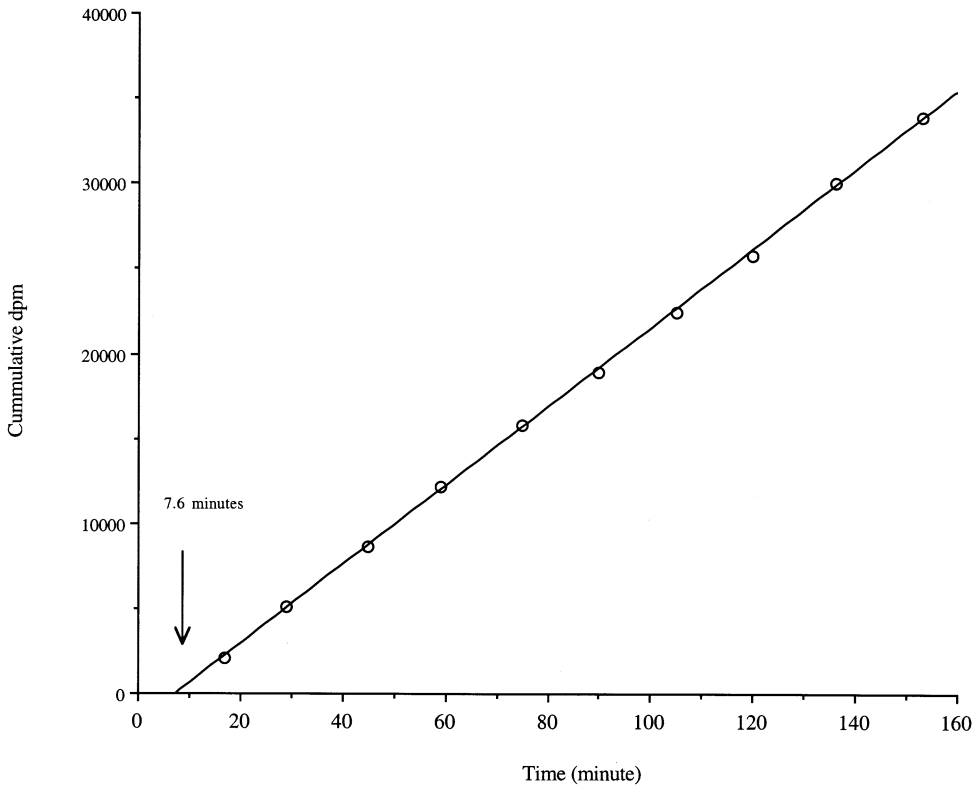

Fig. 2. Representative flux data in a permeation study with ethanol treated HEM (skin sample i). The donor concentration in this permeation experiment was 1.25×10^6 dpm/ml. The slope of the linear regression line is 2.3×10^2 dpm/min.

high. After ethanol treatment, the $h\tau$ values decreased to around 0.1–0.25 cm, corresponding to an approximately seven-fold decrease in the tortuosity of the pore pathways. Delipidization by $CHCl_3$–MeOH (2:1) generally increased the calculated porosity of SC by around 170 times (more than a 1000-fold increase in P values) and decreased the effective thickness to 0.03–0.07 cm, which corresponds to an approximately 20-fold reduction in the tortuosity of the pore pathways in SC. Results from the $CHCl_3$–MeOH pretreatment studies are presented here with the concern that the contribution of the viable epidermis and the Millipore supporting membrane to the total lag time may not be insignificant (as pointed out earlier).

It is noteworthy that the model-deduced τ values (based on $h \approx 27$ μm) in Table 2 seem to be larger than what might be expected from the 'brick and mortar' structure in SC (Michaels et al., 1975; Edwards and Langer, 1994; Heisig et al., 1996; Johnson et al., 1997), when it is assumed that the pore pathway may be associated with the intercellular lipids.

3.5. Results from the 'bottleneck' transport model using data obtained in HEM, EtOH treated HEM and $CHCl_3$–MeOH treated HEM permeation studies

Table 2 also presents the values for the total accessible compartment volume, V_T (where $V_T = jV$), calculated from the 'bottleneck' transport model for SC (0.0029 ± 0.0013 cm^3), ethanol treated SC (0.009 ± 0.005) and $CHCl_3$–MeOH treated SC (0.025 ± 0.014 cm^3). The model-deduced apparent V_T values for ethanol and

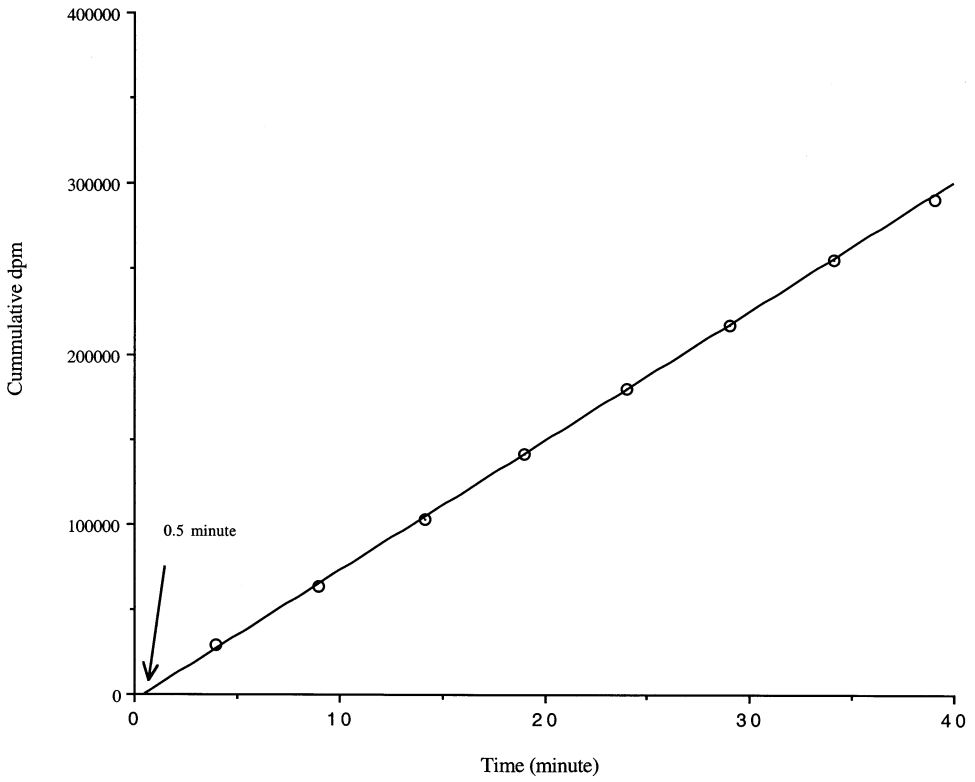

Fig. 3. Representative flux data in a permeation study with chloroform–methanol (2:1, v/v) treated HEM (skin sample n). The donor concentration in this permeation experiment was 1.1×10^6 dpm/ml. The slope of the linear regression line is 7.6×10^3 dpm/min.

$CHCl_3$–MeOH treated SC are several fold larger than those of SC without these treatments. The V_T values for hydrated SC without ethanol or $CHCl_3$–MeOH treatment are around three times larger than the volume increase in SC due to hydration, ΔV_h (0.0009 ± 0.0006 cm^3) where:

$$\Delta V_h = (h_w - h_d)A \quad (10)$$

where h_w is the thickness of wet SC, approximately 27 μm (see Section 3.1), and h_d is the thickness of dry SC, approximately 15 μm (Allenby et al., 1969; Corcuff et al., 1993, 1996; Johnson et al., 1997).

3.6. Trypsin treated HEM permeation study

Table 1 shows HEM data for before and after trypsin treatment. As can be seen here, the permeabilities and lag times of these HEM samples were not significantly affected by trypsin treatment. In preliminary studies, physical inspection of HEM samples and HEM thickness measurement indicated that the viable epidermis layer of HEM was removed after trypsin treatment leaving only the SC behind; in general, the viable epidermal side of HEM changed from dull to shiny, there was a loss of skin pigment, and HEM thickness decreased after trypsin treatment (data not shown). In Tables 1 and 2, results from trypsin treated skin samples, except for the ethanol treated sample k (an outlier here for some unknown reason), are seen not to be significantly different from those without trypsin treatment (skin samples g, h, i and j); this supports the contention that the viable epidermal layer did not contribute significantly to the barrier properties in the permeation of urea for both HEM and ethanol treated HEM. In studies on the barrier properties of tape-stripped

Table 2
Effective thickness ($h\tau$) and porosity (ϵ) determined by the tortuous pathway model and total aqueous accessible compartment volume (V_T) determined by the 'bottleneck' equilibration model of HEM, ethanol treated HEM and $CHCl_3$–MeOH (2:1) treated HEM

Sample	PBS			EtOH treated			$CHCl_3$–MeOH treated		
	$h\tau$ (cm)	ϵ	V_T (cm^3)	$h\tau$ (cm)	ϵ	V_T (cm^3)	$h\tau$ (cm)	ϵ	V_T (cm^3)
a	1.13	0.0041	0.0032	–	–	–	–	–	–
b	1.08	0.0033	0.0024	–	–	–	–	–	–
c	1.01	0.0038	0.0026	–	–	–	–	–	–
d	1.29	0.0033	0.0029	–	–	–	–	–	–
e	1.03	0.0036	0.0026	–	–	–	–	–	–
f	1.15	0.0031	0.0025	–	–	–	–	–	–
g	1.31	0.0050	0.0045	0.15	0.13	0.013	–	–	–
h	1.6	0.0015	0.0017	0.106	0.059	0.0044	–	–	–
i	1.12	0.0040	0.0032	0.16	0.069	0.0077	–	–	–
j	0.47	0.0037	0.0012	0.19	0.085	0.011	–	–	–
k[a]	1.72	0.0010	0.0012	0.020[b]	0.044[b]	0.0006[b]	–	–	–
l[a]	1.44	0.0018	0.0019	0.23	0.064	0.010	–	–	–
m[a]	1.26	0.0024	0.0022	0.22	0.10	0.015	–	–	–
n	0.93	0.0060	0.0038	–	–	–	0.044	0.65	0.020
o	1.35	0.0037	0.0035	–	–	–	0.067	0.96	0.043
p	0.74	0.013	0.0066	–	–	–	0.065	0.67	0.029
q	0.67	0.0067	0.0033	–	–	–	0.026	0.46	0.0091
Mean		0.0041	0.0029		0.079	0.009		0.69	0.025
±S.D.		±0.0027	±0.0013		±0.029	±0.005		±0.21	±0.014

[a] Between the permeation run in PBS and the permeation run after ethanol treatment, HEM were treated with trypsin solution.
[b] No explanation for these results, which are at considerable variance from all other results.

human skin and the human dermis layer, Liu et al. (1994) estimated the permeability of human viable epidermal layer for β-estradiol to be around 2×10^{-4} cm/s. A urea P value of this order of magnitude for the viable epidermis would be large enough that the viable epidermis would not be important in both the HEM and ethanol treated HEM permeation experiments and would be consistent with the present results (Table 1).

4. Discussion

4.1. Error analysis

Errors from extrapolation of the observed 'linear' flux region to the abscissa for lag time determination were estimated by comparing the lag time calculated from theory and the lag time determined by simulation of the extrapolation process under the experimental conditions employed in the present study (see Appendix A). Results from this simulation with typical parameters (effective thickness ≈ 1.25 cm and porosity ≈ 0.005) show that the lag time (T) determined in experiments that assume steady-state after $1.5T$, $2T$ and $3T$ is around 18, 9 and 3% less than the actual theoretical lag time value. Thus, errors in the lag time determination resulting from not attaining steady-state are considered negligible as the length of the permeation runs was generally more than three times the experimental lag times. It should be noted that the above error analysis does not account for random experimental errors which depend on the sampling interval, membrane permeability, the lag time itself, and the number of samples taken, etc.

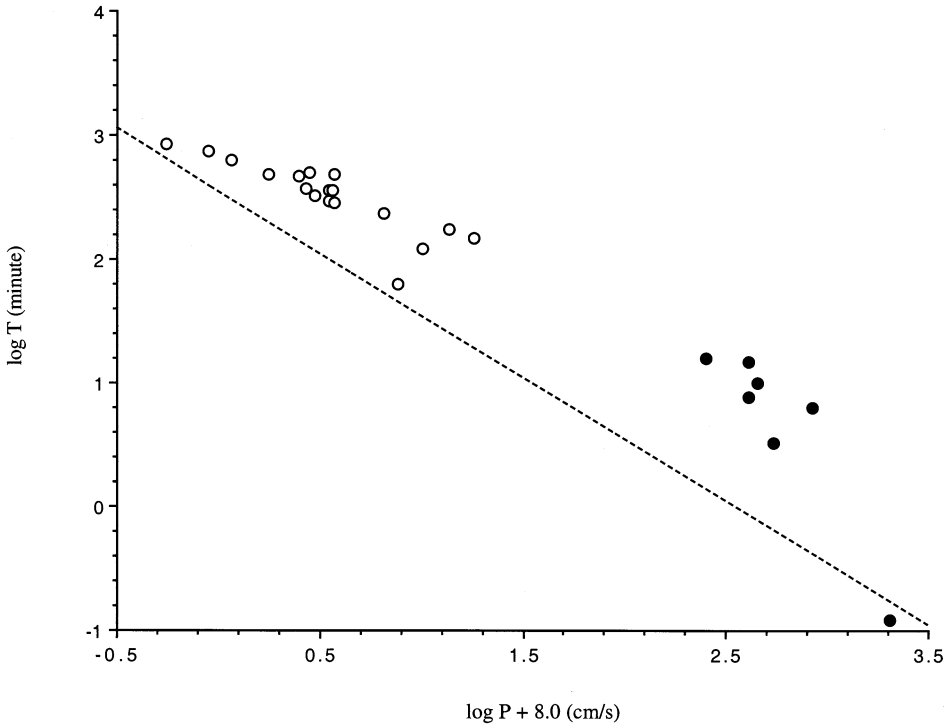

Fig. 4. A relationship between transport lag time (T) and permeability coefficient (P) from experimental data obtained in HEM permeation study, ethanol treated HEM permeation study, and simulation results from the 'bottleneck' equilibration transport model. Model simulation was carried out using the experimental volume increase in SC due to hydration, ΔV_h (i.e. 0.0009 cm^3), as V_T. Symbols: HEM (open circle); ethanol treated HEM (closed circle); model simulation (dotted line).

4.2. Examination of the models

The analysis using Eqs. (3)–(9) have been based on convenient but likely oversimplified models for fully hydrated human SC. The tortuous pathway model and the 'bottleneck' transport models represent, to a large extent, two extreme situations: the former is a homogeneous 'continuum' model and the latter is a homogeneous 'lumped-series' model. Neither of these two models seems to perfectly represent the experimental results as noted in Sections 3.4 and 3.5. If the pore pathway is associated with transport parallel to the lipid bilayers in the hydrated polar/aqueous region of the SC intercellular lipids and if moderate, uniform extent of hydration is allowed, the τ values (of several hundreds) deduced from the tortuous pathway model seem higher than reasonable based on the 'brick and mortar' picture for the SC where tortuosity values of around 4 (e.g. Johnson et al., 1997) to around 25 (e.g. Edwards and Langer, 1994) are indicated depending on the vertical alignment of the corneocytes in the SC. This suggests that the tortuous pathway model (with uniform, moderately hydrated polar regions of the intercellular bilayers) alone might not adequately account for the long lag times observed in the present study. We have also noted that the 'bottleneck' transport model has generally yielded V_T values that are three times larger than the volume change of SC due to hydration. Fig. 4 shows a comparison between the experimental results and the 'bottleneck' model simulation results when the ΔV_h value of 0.0009 cm^3 is used instead of the V_T values given in Table 2. The deviations seen in Fig. 4 are consistent with $\Delta V_h \approx 0.0009$ cm^3 being around three times too small to represent the actual situation. This systematic discrepancy between the 'bottleneck' model predictions (based on $V_T \approx \Delta V_h$) and ex-

perimental results are likely related to the key assumption underpinning the 'bottleneck' model—i.e. the 'lumping' of the transport properties as an alternating series of 'resistance' components and 'well-mixed' compartments. Arguments are now presented to support a model that would likely better represent the observed data and, at the same time, to provide a physical basis for discrepancies observed with the tortuous pathway and the 'bottleneck' transport models.

The proposed model may be viewed as a modified tortuous pathway model or as a modified 'bottleneck' transport model. This more realistic model is considered as having tortuous channels (Eq. (4)) but, because there may be significant access of the permeant to other aqueous compartments associated with the intercellular lipids (van Hal et al., 1996) or with the corneocyte interiors, Eq. (3) will need to be modified to allow for this enhanced local partitioning (Higuchi and Higuchi, 1960; Higuchi, 1967). This scenario would likely be consistent both with the very long lag times observed (Table 1) and with the morphology of fully hydrated SC. This new model would also reconcile the discrepancies found with the 'bottleneck' transport model as, in effect, a lag time contribution from the 'resistive' component of the 'bottleneck' transport model is involved; a smaller V_T value would therefore suffice for this modified 'bottleneck' transport model to better simulate the experimental results. As the amounts of water in the intercellular regions and in the corneocyte regions of hydrated SC are generally of the same order of magnitude (Raykar et al., 1988; see SC aqueous volume fraction estimated in Section 3.5), partitioning of polar permeants between the two regions could be comparable. A preliminary quantitative examination of this proposed model combining the tortuous pathway model and the 'bottleneck' transport model in series shows that a several fold decrease in the effective tortuosity in the tortuous pathway portion of the model and a significant decrease in the total accessible aqueous volume in the 'bottleneck' part of the model can be easily accommodated.

It should be noted that the observed lag times may also be interpreted by other more complicated models with the complicated morphology of SC. Also, we have assumed homogeneity of the membrane; i.e. the effects of possible variabilities in the transport properties in the direction of transport or parallel to the membrane have not been considered. Nevertheless, the model proposed here appears to adequately account for the experimental HEM permeability behavior for urea as a representative polar permeant.

4.3. Nature of SC pore pathways

Fig. 5 shows a correlation between the permeability and electrical resistance for SC and ethanol treated SC. The correlation with a slope of -1.0 suggests that the transport pathways of HEM for urea are related to those for the conducting ions in PBS and that the pore pathways behave similarly to a porous membrane. However, a slope of -1.0 might not have been expected had the size of the polar permeant molecule been very different from those of the conducting ions for transport across a restricted pore pathway in HEM (Li et al., 1997, 1998).

Previously, the physical properties of the pore pathways in human and rat skin have been characterized using model polar permeants, and, in these studies, the effective pore radii for the pore pathways in human and rat SC were estimated to be around 15–25 Å (Peck et al., 1994) and 4–16 Å (Hatanaka et al., 1994), respectively. The nanometer order effective pore radii suggest the involvement of structures (or altered structures due to hydration) that have significantly smaller dimensions than those of the macropore structures (e.g. appendages and hair follicles) in the transport of polar permeants in SC. Studies on the effects of temperature upon the transport of polar permeants show an activation energy of around 7 kcal/mol for the transport of these permeants (Peck et al., 1995); this suggests that the pore pathway, in general, behaves like that of ideal aqueous pores (activation energy around 4–5 kcal/mol), in contrast to the lipoidal nature of the transport pathways for lipophilic permeants. New information obtained in the present investigation has provided further mechanistic insights into the nature of the pore pathway in SC.

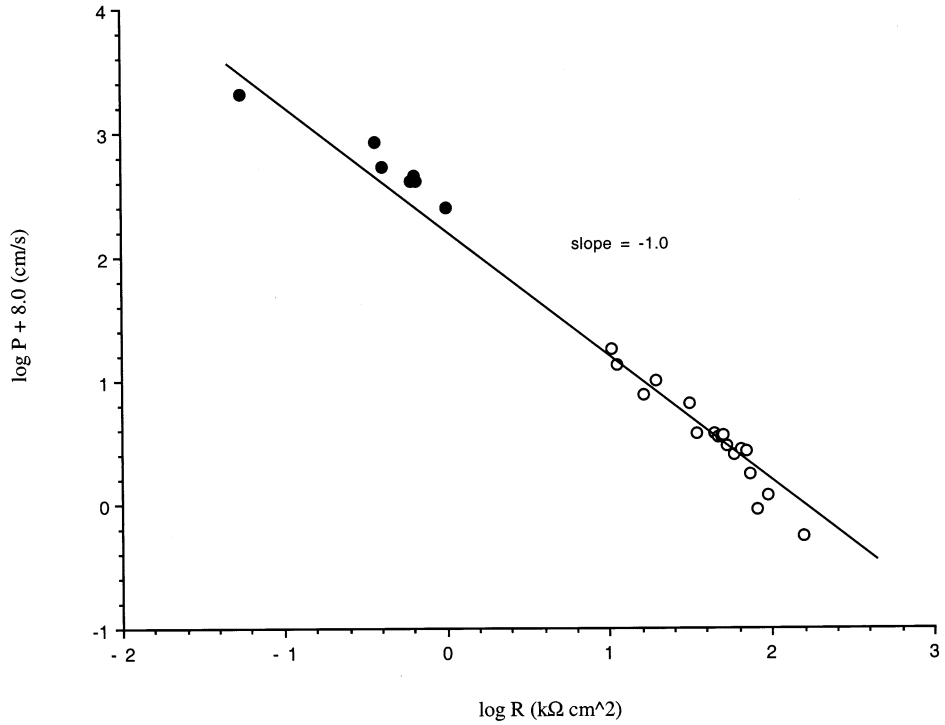

Fig. 5. A correlation ($r^2 = 0.985$) of permeability coefficient (P) and electrical resistance (R) of HEM (open symbols) and ethanol treated HEM (closed symbols). The slope of the line is -1.0.

In the present study, the transport lag times for urea of the order of hundreds of minutes (Table 1) suggests the pore pathway being highly tortuous in nature such as that expected from the 'brick and mortar' structure and the large accessible volume of aqueous compartments in SC for transport.

The hypothesis of a relationship between the 'brick and mortar' structure of SC and the pore pathway is consistent with results from studies using microscopy techniques to trace the locations of ions in SC (Sharata and Burnette, 1988; Bodde et al., 1991). In these microscopy studies, ions are observed to be located along the intercellular lipids in SC during transport. However, a caveat here is that such techniques cannot distinguish between permeant binding to SC from the flux density of permeants along different transport routes.

An interesting observation in the present study was a relationship between the electrical resistance of HEM (R) and its transport lag time (T) as shown in Fig. 6. Literature (Kasting and Bowman, 1990; Peck et al., 1995) suggests that HEM with low resistance ($\lesssim 20$ kΩ cm^2) may be indicative of membrane defects and/or macropore involvement in the transport of polar permeants. Thus, the relationship in Fig. 6 is consistent with the hypothesis that skin samples of high resistance have less appendage routes or less damage, and, therefore, the transport of polar permeants is predominantly via the tortuous pathways associated with the polar regions of the intercellular lipids in the SC. Another possible explanation for this relationship is the variation in SC thickness (h). Thickness alone, however, may be expected to yield a stronger dependence of T on R (see Eqs. (3) and (4) and Fig. 5). This dependence is not apparent in Fig. 6.

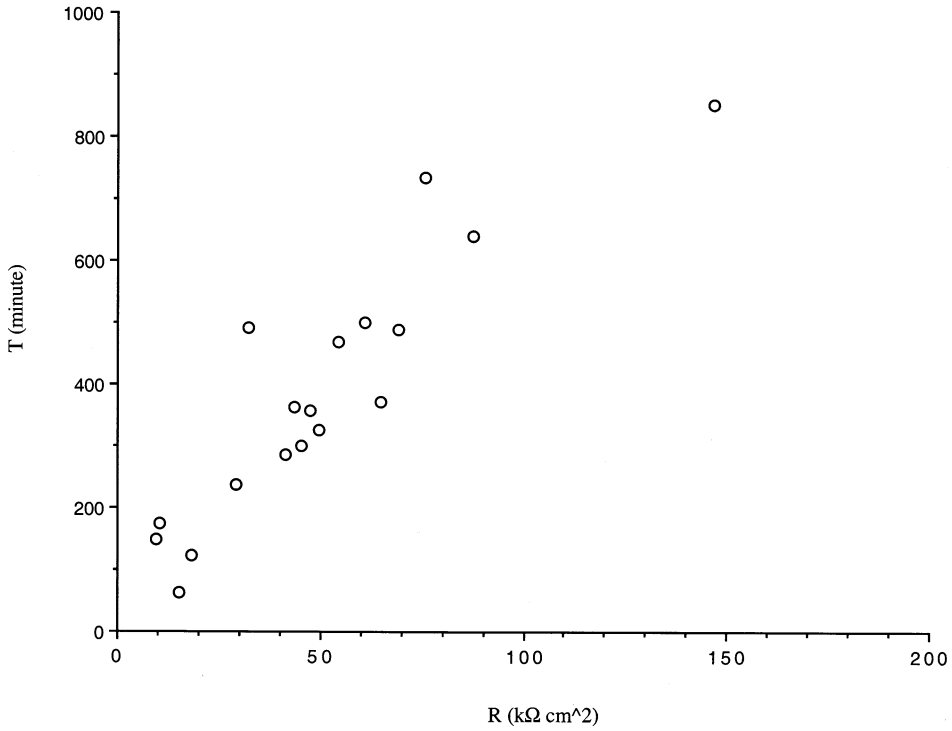

Fig. 6. A relationship between transport lag time (T) and HEM electrical resistance (R) from the data obtained with untreated HEM.

4.4. Mechanistic insights of SC pore pathways from ethanol and $CHCl_3$–MeOH pretreatment studies

The increase in the permeability of SC and the decrease in its transport lag time after ethanol and $CHCl_3$–MeOH treatments support the hypothesis that SC barrier properties (i.e. porosity and tortuosity) are associated with the polar regions of the SC intercellular lipids for the transport of polar permeants. The pore pathway may be viewed as the transport along the polar/aqueous regions between bilayers of the intercellular lipids. It has been suggested that ethanol and $CHCl_3$–MeOH treatments remove SC intercellular lipids (Gray and Yardley, 1975; Bommannan et al., 1991). The remaining high tortuosity after ethanol treatment suggests that permeants may continue to travel primarily around the corneocytes; the highly resistive barriers around the corneocytes (Wertz and Downing, 1986) may largely remain intact after ethanol treatment. Further delipidization by $CHCl_3$–MeOH may provide pathways through these corneocytes (or their remnants), and this situation may thus correspond to greatly reduced tortuosity.

It is noteworthy that the correlation between HEM electrical resistance and the permeability of HEM for urea was essentially sustained after ethanol treatment (Fig. 5). The SC was significantly altered by ethanol delipidization as evidenced by both a large increase in porosity and an apparent decrease in the effective pore size (Peck et al., 1994). However, the correlation seen here is independent of the alteration, suggesting that urea transport likely followed the same pathways as the conducting ions for both SC and ethanol treated SC. Both SC and ethanol treated SC behave as ideal porous membranes for the transport of urea and presumably for other polar permeants.

The analysis in the present study with the lag time data obtained from SC, ethanol treated SC, and $CHCl_3$–MeOH treated SC has demonstrated the value of lag time data in gaining useful insights into the nature of the pore pathway of fully hydrated human skin.

Acknowledgements

This research is supported by NIH Grant GM 43181 and a predoctoral fellowship in pharmaceutics from the Pharmaceutical Research and Manufacturers of America Foundation. The authors thank TheraTech Inc., Salt Lake City, UT, for supplying the skin samples and Professor Jeffrey L. Fox for helpful discussion.

Appendix A. Error analysis using a non-steady state flux model

The cumulative amount (Q) of permeants in the receiver chamber was derived from Fick's law (e.g. Higuchi and Higuchi, 1960):

$$Q = \frac{HDC_D}{\tau h} t + \frac{2HDC_D}{\tau h} \sum_{m=1}^{\infty} \frac{(-1)^m}{m^2} \frac{(\tau h)^2}{HD\pi^2} \times \left[1 - \exp\left(\frac{-HDm^2\pi^2 t}{(\tau h)^2}\right)\right] \quad \text{(A1)}$$

where H is the hindrance factor, D is the diffusion coefficient, τh is the effective thickness of the membrane, t is time, and C_D is the concentration in the donor chamber. Q vs. t plots were obtained from simulation of Eq. (A1) using a spreadsheet and graphic software. The theoretical lag time (Eq. (3)) was compared with lag time determined by extrapolating data from different regions in the plots (from $1.5 \times$ lag time to $2 \times$ lag time, from $2 \times$ lag time to $3 \times$ lag time, and $3 \times$ lag time to $4 \times$ lag time) to the abscissa.

References

Ackermann, C., Flynn, G.L., Smith, W.M., 1987. Ether–water partitioning and permeability through nude mouse skin in vitro. II. Hydrocortisione 21-n-alkyl-esters, alkanols and hydrophilic compounds. Int. J. Pharm. 36, 67–71.

Allenby, A.C., Fletcher, J., Schock, C., Tees, T.F.S., 1969. The effect of heat, pH and organic solvents on the electrical impedance and permeability of excised human skin. Br. J. Dermatol. 81 (Suppl. 4), 31–39.

Bodde, H.E., Van den Brink, I., Koerten, H.K., de Haan, F.H.N., 1991. Visualization of in vitro percutaneous penetration of mercuric chloride; transport through the intercellular space versus cellular uptake through desmosomes. J. Control. Release 15, 227–236.

Bommannan, D., Potts, R.O., Guy, R.H., 1991. Examination of the effect of ethanol on human stratum corneum in vivo using infrared spectroscopy. J. Control. Release 16, 299–304.

Corcuff, P., Bertrand, C., Leveque, J.L., 1993. Morphometry of human epidermis in vivo by real-time confocal microscopy. Arch. Dermatol. Res. 285, 475–481.

Corcuff, P., Gonnord, G., Pierard, G.E., Leveque, J.L., 1996. In vivo confocal microscopy of human skin: a new design for cosmetology and dermatology. Scanning 18, 351–355.

Edwards, D.A., Langer, R., 1994. A linear theory of transdermal transport phenomena. J. Pharm. Sci. 83, 1315–1334.

Flynn, G.L., 1990. Physicochemical determinants of skin absorption. In: Gerrity, T.R., Henry, C.J. (Eds.), Principles of Route to Route Extrapolation of Risk Assessment. Elsevier, New York, pp. 93–127.

Flynn, G.L., Yalkowsky, S.H., Roseman, T.J., 1974. Mass transport phenomena and models: theoretical concepts. J. Pharm. Sci. 63, 479–510.

Goto, S., Uchida, T., Lee, C.K., Yasutake, T., Zhang, J.-B., 1993. Effect of various vehicles on ketoprofen permeation across excised hairless mouse skin. J. Pharm. Sci. 82, 959–963.

Gray, G.M., Yardley, H.J., 1975. Lipid compositions of cells isolated from pig, human, and rat epidermis. J. Lipid Res. 16, 434–440.

Guy, R.H., Hadgraft, J., 1988. Physicochemical aspects of percutaneous penetration and its enhancement. J. Pharm. Res. 5, 753–758.

Hatanaka, T., Shimoyama, M., Sugibayashi, K., Morimoto, Y., 1993. Effect of vehicle on the skin permeability of drugs: polyethylene glycol 400–water and ethanol–water binary solvents. J. Control. Release 23, 247–260.

Hatanaka, T., Manabe, E., Sugibayashi, K., Morimoto, Y., 1994. An application of the hydrodynamic pore theory to percutaneous absorption of drugs. Pharm. Res. 11, 654–658.

Heisig, M., Lieckfeldt, R., Wittum, G., Mazurkevich, G., Lee, G., 1996. Non steady-state descriptions of drug permeation through stratum corneum. I. The biphasic brick-and-mortar model. Pharm. Res. 13, 421–426.

Higuchi, W.I., 1967. Diffusional models useful in biopharmaceutics: drug release rate processes. J. Pharm. Sci. 56, 315–324.

Higuchi, W.I., Higuchi, T., 1960. Theoretical analysis of diffusional movement through heterogeneous barriers. J. Am. Pharm. Assoc. 49, 598–606.

Holbrook, K.A., Odland, G.F., 1974. Regional differences in the thickness (cell layers) of the human stratum corneum: an ultrastructural analysis. J. Invest. Dermatol. 62, 415–422.

Johnson, M.E., Blankschtein, D., Langer, R., 1997. Evaluation of solute permeation through the stratum corneum: lateral bilayer diffusion as the primary transport mechanism. J. Pharm. Sci. 86, 1162–1172.

Kasting, G.B., Bowman, L.A., 1990. DC electrical properties of frozen, excised human skin. Pharm. Res. 7, 134–143.

Li, S.K., Ghanem, A.-H., Peck, K.D., Higuchi, W.I., 1997. Iontophoretic transport across a synthetic membrane and human epidermal membrane: a study of the effects of permeant charge. J. Pharm. Sci. 86, 680–689.

Li, S.K., Ghanem, A.-H., Peck, K.D., Higuchi, W.I., 1998. Characterization of the transport pathways induced during low to moderate voltage iontophoresis in human epidermal membrane. J. Pharm. Sci. 87, 40–48.

Liu, P., Higuchi, W.I., Ghanem, A.-H., Good, W.R., 1994. Transport of β-estradiol in freshly excised human skin in vitro: diffusion and metabolism in each skin layer. Pharm. Res. 11, 1777–1784.

Loftsson, T., Bodor, N., 1981. Improved delivery through biological membranes. X: Percutaneous absorption and metabolism of methylsulfinylmethyl 2-acetoxy benzoate and related aspirin prodrugs. J. Pharm. Sci. 70, 756–758.

Martin, A.N., Bustamante, P., 1993. Physical Pharmacy: Physical Chemical Principles in the Pharmaceutical Sciences. Philadelphia, Lea and Febiger, Ch. 13.

Michaels, A.S., Chandrasekaran, S.K., Shaw, J.E., 1975. Drug permeation through skin: theory and in vitro experimental measurement. AIChE J. 21, 985–996.

Morimoto, Y., Hatanaka, T., Sugibayashi, K., Omiya, H., 1992. Prediction of skin permeability of drugs: comparison of human and hairless rat skin. J. Pharm. Pharmacol. 44, 634–639.

Peck, K.D., Ghanem, A.-H., Higuchi, W.I., Srinivasan, V., 1993. Improved stability of the human epidermal membrane during successive permeability experiments. Int. J. Pharm. 98, 141–147.

Peck, K.D., Ghanem, A.-H., Higuchi, W.I., 1994. Hindered diffusion of polar molecules through and effective pore radii estimates of intact and ethanol treated human epidermal membrane. Pharm. Res. 11, 1306–1314.

Peck, K.D., Ghanem, A.-H., Higuchi, W.I, 1995. The effect of temperature upon the permeation of polar and ionic solutes through human epidermal membrane. J. Pharm. Sci. 84, 975–982.

Pershing, L.K., Lambert, L.D., Knutson, K., 1990. Mechanism of ethanol-enhanced estradiol permeation across human skin in vivo. Pharm. Res. 7, 170–175.

Potts, R.O., Guy, R.H., 1992. Predicting skin permeability. Pharm. Res. 9, 663–669.

Potts, R.O., Guy, R.H., 1995. A predictive algorithm for skin permeability: the effects of molecular size and hydrogen bond activity. Pharm. Res. 12, 1628–1633.

Raykar, P.V., Fung, M.C., Anderson, B.D., 1988. The role of protein and lipid domains in the uptake of solutes by human stratum corneum. Pharm. Res. 5, 140–150.

Roberts, M.S., Anderson, R.A., Swarbrick, J., 1977. Permeability of human epidermis to phenolic compounds. J. Pharm. Pharmacol. 29, 677–683.

Sharata, H., Burnette, R.R., 1988. Effect of dipolar aprotic permeability enhancers on the basal stratum corneum. J. Pharm. Sci. 77, 27–32.

Sims, S.M., Higuchi, W.I., Srinivasan, V., 1991. Skin alteration and convective solvent flow effects during iontophoresis: I. Neutral solute transport across human skin. Int. J. Pharm. 69, 109–121.

Srinivasan, V., Higuchi, W.I., Su, M.-H., 1989. Baseline studies with the four-electrode system: the effect of skin permeability increase and water transport on the flux of a model uncharged solute during iontophoresis. J. Control. Release 10, 157–165.

Tojo, K., Chiang, C.C., Chien, Y.W., 1987. Drug permeation across the skin: effect of penetrant hydrophilicity. J. Pharm. Sci. 76, 123–126.

van Hal, D.A., Jeremiasse, E., Junginger, H.E., Spies, F., Bouwstra, J.A., 1996. Structure of fully hydrated human stratum corneum: a freeze-fracture electron microscopy study. J. Invest. Dermatol. 106, 89–95.

Wertz, P.W., Downing, D.T., 1986. Covalent attachment of ω-hydroxyacid derivatives to epidermal macromolecules: a preliminary characterization. Biochem. Biophys. Res. Commun. 137, 992–997.